PAPER

A theoretical study of substitutional boron–nitrogen clusters in diamond

View the article online for updates and enhancements.

IOP ebooks™

Bringing you innovative digital publishing with leading voices to create your essential collection of books in STEM research.

Start exploring the collection - download the first chapter of every title for free.

A theoretical study of substitutional boron–nitrogen clusters in diamond

Alex Croot[1] , **M Zamir Othman**[2], **Sergio Conejeros**[3] , **Neil A Fox**[1,4]
and **Neil L Allan**[4]

[1] H H Wills Physics Laboratory, University of Bristol, Tyndall Avenue, Bristol BS8 1TL,
United Kingdom
[2] Faculty of Science and Technology, Universiti Sains Islam Malaysia (USIM), Bandar Baru, Nilai,
71800 Nilai, Negeri Sembilan, Malaysia
[3] Departamento de Química, Universidad Católica del Norte, Av. Angamos 0610, Antofagasta,
124000, Chile
[4] School of Chemistry, University of Bristol, Cantock's Close, Bristol BS8 1TS, United Kingdom

E-mail: a.croot@bristol.ac.uk

CrossMark

Abstract
Substitutional clusters of multiple light element dopants are a promising route to the elusive
shallow donor in diamond. To understand the behaviour of co-dopants, this report presents
an extensive first principles study of possible clusters of boron and nitrogen. We use periodic
hybrid density functional calculations to predict the geometry, stability and electronic
excitation energies of a range of clusters containing up to five N and/or B atoms. Excitation
energies from hybrid calculations are compared to those from the empirical marker method,
and are in good agreement.

When a boron-rich or nitrogen-rich cluster consists of three to five atoms, the minority
dopant element—a nitrogen or boron atom respectively—can be in either a central or
peripheral position. We find B-rich clusters are most stable when N sits centrally, whereas
N-rich clusters are most stable with B in a peripheral position. In the former case, excitation
energies mimic those of the single boron acceptor, while the latter produce deep levels in
the band-gap. Implications for probable clusters that would arise in high-pressure high-
temperature co-doped diamond and their properties are discussed.

Keywords: diamond, DFT, co-doping, clusters, hybrid

(Some figures may appear in colour only in the online journal)

1. Introduction

Throughout the last few decades doping of diamond has been
one-sided, with boron an easily incorporated, moderately
shallow acceptor while nitrogen fails to provide a shallow
donor state [1, 2]. Various attempts have been made to pro-
duce a conducting n-type material with phosphorus so far the
most experimentally successful [3]. Even though it lies below
nitrogen in the periodic table, the phosphorus donor level is
still as much as 0.6 eV below the conduction band minimum
(CBM). With its larger size also leading to more defective
diamond and hence conductivity problems, phosphorus is
proving not to be the donor dopant required to produce n-type

diamond material. The unfortunate trade-off for any heavier
element, expected to provide a shallower donor level than
phosphorus, is even higher formation energies, poorer quality
diamond and lower conductivity material.

Attention has turned toward combinations of small atoms
arranged in clusters as a means of producing a suitable donor
[4–6]. This so-called *co-doping* may have the advantage that
appropriate arrangements of lighter, more easily incorporated
atoms could provide the desired characteristics for a useful
n-type material.

Theoretical work has provided insight into various combi-
nations of elements, highlighting clusters that add one elec-
tron to the diamond lattice such as BN_2 [7], Si_4N [8] and LiN_4

[9]. It is clear from intensive research that care must be taken when studying these clusters, both theoretically—e.g. supercell size [10]—and from an experimental point of view—e.g. ease of fabrication [11]. The predicted stability, or binding energy, of these clusters is often high since, thanks to electronegativity and size effects, co-dopants couple strongly [12].

Little experimental work has been carried out to realise these shallow donor clusters, with the primary method of controlled doped diamond synthesis, chemical vapour deposition (CVD) [13], unlikely to result in a high concentration of aggregated dopants. While high incorporation efficiencies can be achieved, e.g. with boron [14], the growth temperatures are most often far below those at which dopants diffuse at any significant rate [15]. The likelihood of incorporation of multiple dopants in adjacent positions is low, so the concentration of clusters is certainly lower than that of isolated dopant atoms, precluding their detection. Nevertheless, attempts have been made to introduce multiple species into diamond, both during CVD [16–20] and post-synthesis [21–23].

The high temperatures involved in high-pressure high-temperature (HPHT) growth and annealing facilitate dopant migration, with annealing studies showing creation of large binding energy cluster defects such as A- and B-centres: a pair of N atoms and four N atoms surrounding a vacancy respectively [24]. Since this process allows formation of complex nitrogen-vacancy clusters, it may be the most promising route to formation of clusters more useful for n-type diamond material.

The two most common diamond dopants, boron and nitrogen, have been shown to associate in HPHT diamond, with the split-interstitial pair being studied both experimentally [25] and theoretically [26]. Furthermore, co-doping of diamond with boron and nitrogen during HPHT synthesis has recently been demonstrated [27–29]. X-ray photoelectron and infra-red spectroscopy of the grown samples show the two dopant species are in fact in adjacent positions, but the exact nature of any complex defects is unclear.

If produced by HPHT, some of the electronically promising clusters predicted to date will be outnumbered by others of higher stability. An example of this is the N–B–N (or BN$_2$) cluster since density functional theory (DFT) calculations predict that a B–N–N cluster (comprising a central N coordinated to one N and one B) is theoretically more stable by 0.5 eV [30]. In fact, there could be a range of defects with varied stability and properties that combine two elements, but many of the studies performed to date focus their attention on a limited set of the most promising clusters.

Hu *et al* [31] studied clusters of boron and nitrogen in diamond by classical molecular dynamics simulations with Tersoff potentials, but the study failed to reproduce the experimental symmetry of the substitutional nitrogen (C-) centre, predicting it to be tetrahedral with four elongated bonds compared to those of pure diamond. Experimentally the nitrogen centre is known to have C_{3v} symmetry with one elongated and three shortened bonds [32]. With a prototypical defect such as this [33] incorrectly modelled, to date there has been no satisfactory computational survey of the possible boron-nitrogen substitional defects that could be present in HPHT diamond.

Furthermore, the electronic behaviour of predicted clusters is as yet unexplored.

To begin to understand co-doping as a method of altering the properties of diamond, an extensive survey of the possible combinations of dopants is required. This report presents an *ab initio* study of boron-nitrogen clusters in diamond, with both nitrogen-rich and boron-rich complexes considered. Both the energetics and electronic properties of these systems are evaluated and discussed in terms of their probable existence in HPHT material.

2. Computational methods

Spin polarised all-electron electronic structure calculations were performed using the CRYSTAL14 program [34] on 512-atom diamond supercells using periodic boundary conditions. Exchange and correlation were treated by the revised hybrid DFT Hartree–Fock functional of Heyd, Scuseria and Ernzerhof (HSE-06) [35]. For carbon we use a 6-21G∗ basis set [36] of 10 Gaussian functions of s, sp and d symmetry. For boron and nitrogen impurities a detailed polarisation quality pob-TZVP basis set [37] was employed, each with 17 Gaussian functions of s, p and d symmetry. For the 512-atom supercell, a converged Monkhurst–Pack [38] grid of $2 \times 2 \times 2$ special k-points sampled the Brillouin zone. During geometry optimisation (via the BFGS scheme [39]) the lattice parameter was fixed at that of the pure diamond supercell and the atoms allowed to relax with substitutional dopants in place of carbon atoms until the system energy changed by less than 10^{-7} Hartree per step. The coulomb and exchange series overlap integral thresholds were set to 10^{-7} and 10^{-14}. Calculations of this type on pure diamond yield bond lengths of 1.55 Å and a band-gap of 5.2 eV.

In this study, ground-spin state structural analysis takes the form of symmetry, bond lengths and binding energies, alongside the energy of formation as defined by:

$$E_{Fm} = E_{defect} + nE_C - \left(E_p + \sum_n \mu_i\right) \quad (1)$$

where E_{defect} is the energy of a supercell containing a geometry-optimised neutral defect or cluster; nE_C is the energy of n carbon atoms removed by substitution of n foreign atoms into the diamond lattice; E_p is the energy of the perfect (undefective) diamond supercell; μ_i is the energy of each of the n impurity atoms, calculated from standard states.

The binding energy, E_b, indicates the interaction of two or more dopants within the lattice, defined as:

$$E_b = E_{Fm,defect} - \sum_n E_{Fm,iso} \quad (2)$$

where $E_{Fm,defect}$ is the formation energy of the defect cluster and $E_{Fm,iso}$ is the formation energy of each isolated constituent impurity. Here we use the convention that E_b is negative for bound systems.

Facile calculations of the excitation energy μ_e of electron donor and acceptor impurities are hampered by a combination of limited supercell sizes causing effective dopant
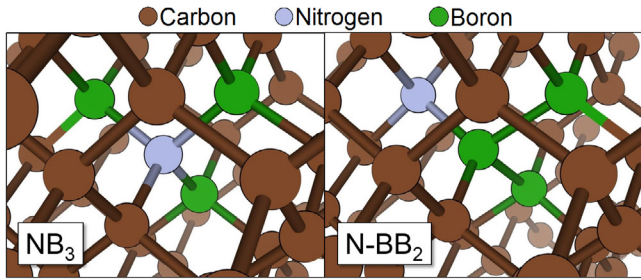
Figure 1. Two stoichiometrically identical but structurally distinct clusters, NB$_3$ and N–BB$_2$. The former is an example of a 'symmetric' boron-rich cluster in which the minority foreign (N) atom is in a central position, and the latter an example 'asymmetric' cluster in which the minority foreign atom is in a peripheral position.

concentrations in the region of thousands of parts per million, and the inherent limitation of exchange functionals in DFT underestimating the band-gap [40]. The use, in this work, of large supercells and hybrid functionals that incorporate part of the Fock exchange energy mitigates this issue somewhat. This allows many systems to be adequately analysed from their density of states (DOS) spectra. Nevertheless, the problem remains for defects with small μ_e; for this reason we compare the DOS results from CRYSTAL14 with results of the *empirical marker method* (EMM), which has been successfully used to compare activation energies of diamond dopants, dopant pairs and multi-dopant clusters [12, 41].

To carry out the EMM, we use the generalised gradient approximation (GGA) of Perdew, Burke and Ernzerhof [42] as implemented by the CASTEP code [43]. The calculation parameters were, where possible, the same as those of the HSE-06 calculations as outlined above, but with a planewave valence basis set of energy up to 800 eV, and ultra-soft core electron pseudopotentials [44]. Due to its large basis set, CASTEP is unable to undertake hybrid functional calculations for these systems, however it does provide a good confirmation of the structural results and a means to compare neutral charge states with positive or negative charge states of a supercell. Using charge calculations, the EMM provides a simple and effective indicator of the acceptor or donor (d) level by comparison to a reference (r) state:

$$\mu_{e,d} = \mu_{e,r} - [(E_d^0 - E_d^+) - (E_r^0 - E_r^+)] \tag{3}$$

where $\mu_{e,d}$ and $\mu_{e,r}$ refer to the excitation energy of the dopant and reference respectively, and E^0 and E^+ the energy of the neutral and charged state respectively. Equation (3) is for a donor, giving positively charged states, but the method is equivalent for acceptors in negatively charged states. The 'markers' used here for acceptors and donors are boron and nitrogen respectively, owing to their similar values of μ_e to many of the examined clusters.

3. Results and discussion

The notation used here for identifying a cluster is similar to that used by previous researchers [12]. For example the A-centre,
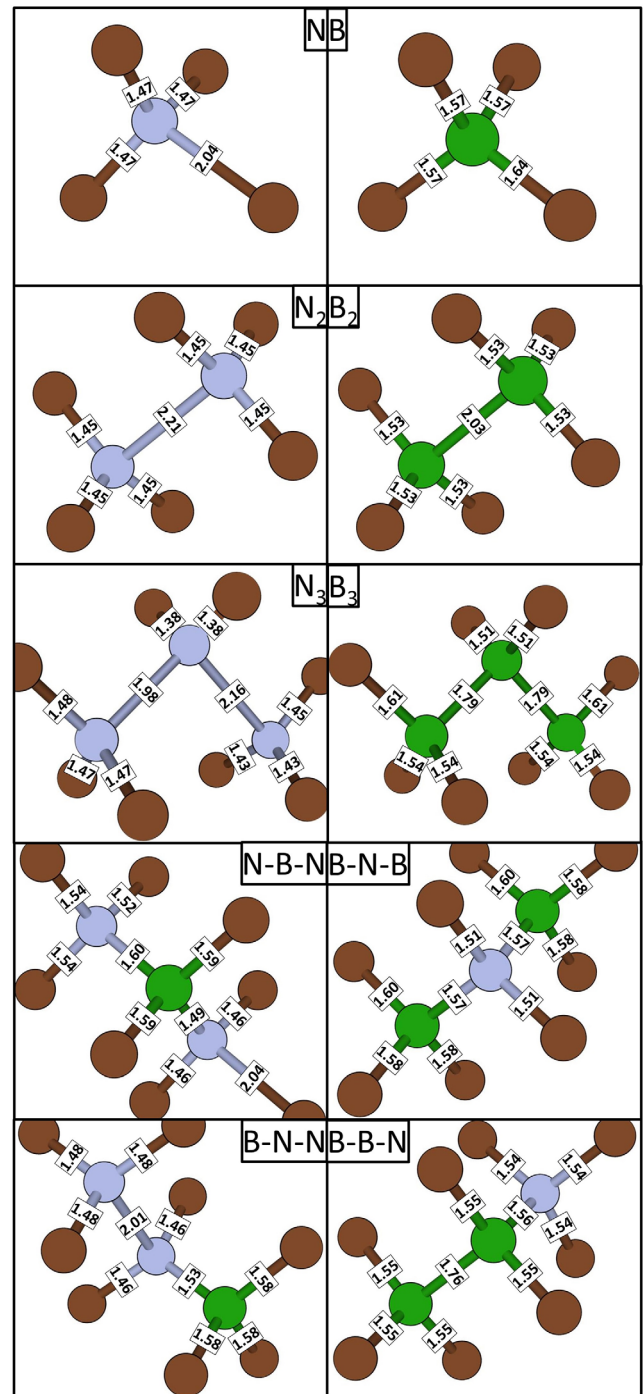
Figure 2. Bond lengths (Å) of B- and N-rich clusters with $n \leqslant 3$. All separations involving dopant atoms (i.e. all but C–C) are shown.

or nitrogen substitutional pair, is denoted N$_2$. Additionally, to distinguish between clusters of equal stoichiometry but distinct atomic arrangement, some clusters are denoted in a form similar to that for B–N–N, avoiding confusion with BN$_2$, which is itself labelled N–B–N. Clusters of equal stoichiometry but differing atomic arrangement are distinguishable by the terms 'symmetric' and 'asymmetric'. A further stoichiometric pair is presented figure 1.
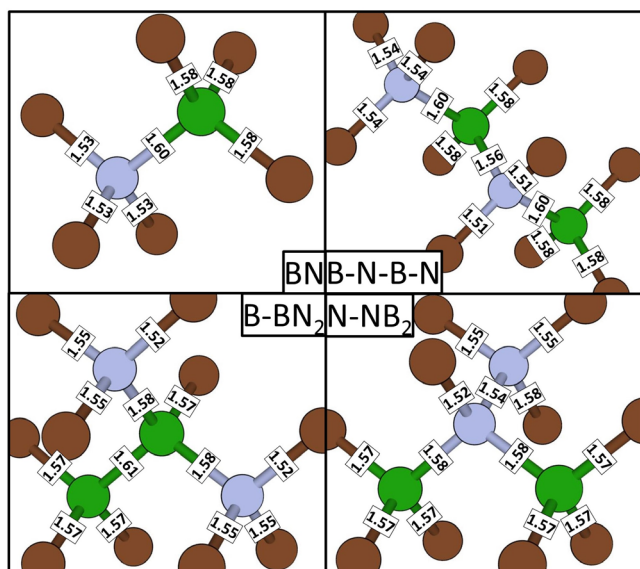
Figure 3. Bond lengths (Å) of equal boron and nitrogen clusters with $n = 2$ and 4. All separations involving dopant atoms (i.e. all but C–C) are shown.

3.1. Defect structures

Figures 2–4 show the HSE-06 boron–nitrogen cluster structures, with a summary of the data shown in table 1. Before geometry relaxation, slightly off-setting the atomic position from the undefective lattice position avoids dopants relaxing into geometric local energy minima. For the isolated nitrogen defect this procedure yields the well-known C_{3v} symmetric state in which one N–C bond is elongated relative to the perfect diamond bond length (C–C_p = 1.55 Å) to 2.04 Å and the other three shorten to 1.47 Å, reflecting the 'lone pair' of electrons on sp^3 hybridised N.

A similar C_{3v} relaxation occurs for single substitutional boron, but with a slight elongation compared to C–C_p even in the shorter three bonds due to the large covalent radius of boron. That said, all changes in bond lengths for the boron dopant are minor.

The same reduction in symmetry does not occur for homonuclear pairs of boron or nitrogen, both of which retain D_{3d} symmetry. The N–C bonds in N_2 are further contracted compared to those of N at 1.45 Å, reflecting a strong repulsion of the lone pairs on the two nitrogen atoms, 2.21 Å apart. A repulsion is also present in B_2, with a B–B bond length of 2.03 Å.

While the homonuclear pairs repel, the heteronuclear pair BN, which is isoelectronic with CC, causes little movement from the intrinsic lattice positions, with the B–N bond only longer than C–C_p by 3%. Owing to the satisfaction of valencies in the BN pair, the bonds from B and N to the surrounding carbon atoms are far closer in length to C–C_p.

Unlike some previous authors [7, 45] the present hybrid calculations find the symmetry of N–B–N to be C_s rather than C_{3v}, as in the unrelaxed case. This symmetry lowering is due to an elongation of a carbon–nitrogen bond on one nitrogen atom, causing a surrounding distortion much like that for N.
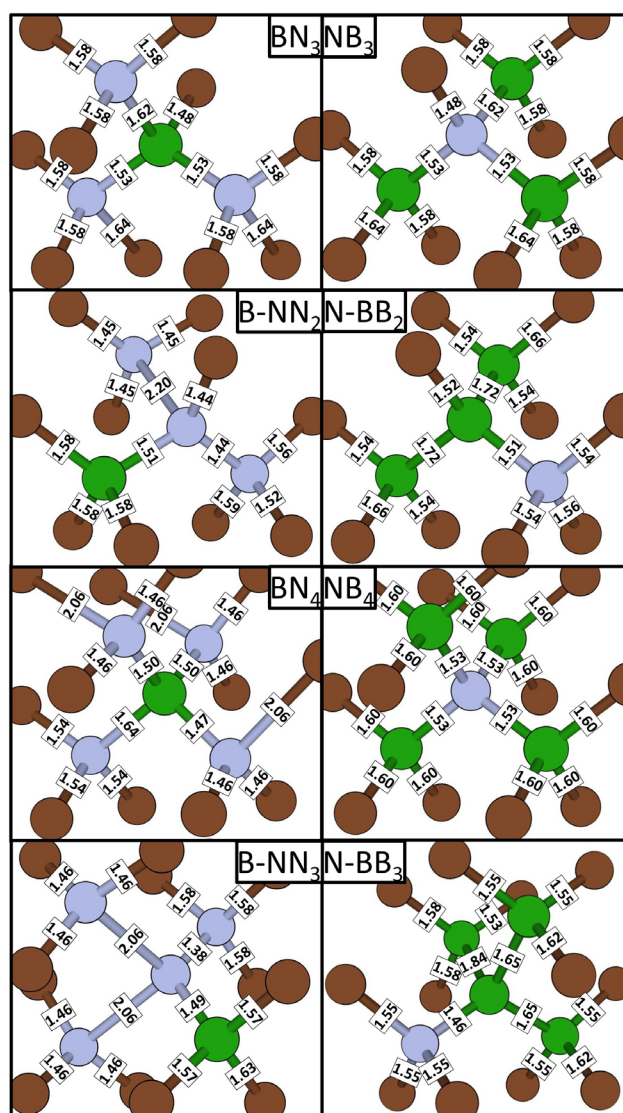
Figure 4. Bond lengths (Å) of B- and N-rich clusters with $n = 4$ and 5. All separations involving dopant atoms (i.e. all but C–C) are shown.

The N–B–N centre may be considered as a 'separate' N adjacent to a valence-satisfied BN. Similarly, in the B–N–N centre the outer nitrogen behaves much like a single N, with its three carbon bonds shorter than C–C_p by 4% and the remaining bond (to nitrogen) longer by 30%, 2.01 Å.

Unlike the nitrogen-rich three-atom clusters, B–N–B and B–B–N are vastly less structurally different from intrinsic diamond itself with a maximum X–C bond length change of 3% relative to C–C_p and the inter-boron bond in B–B–N (1.76 Å) being less than half as extended as that in B_2 (2.03 Å). Relative to C–C_p, the boron–carbon bonds in B–N–B are extended by only around 1%, resulting in a relaxed geometry with C_{2v} symmetry.

Of the clusters containing two nitrogen atoms and two boron atoms, B–BN_2, N–NB_2 and B–N–B–N, little structural change from perfect lattice positions is apparent. All have low symmetry, C_s, simply due to their atomic arrangement. Addition of a compensating atom to the three-atom clusters clearly reduces the resulting structural changes considerably.

Table 1. Lowest energy spin-state symmetry and structural results for the clusters examined by HSE-06 calculations. Symmetries before and after the geometries are optimised from perfect lattice positions to their ground states are denoted Unopt and Opt respectively. Bond lengths are given in units of the calculated perfect diamond carbon–carbon bond length $C–C_p$, 1.55 Å, followed by a bracket containing the number of bonds of the given length stemming from each central atom: for example '1.02 (3,1)' under the C–B heading refers to four bonds 2% longer than those of perfect diamond, three originating at one boron atom and one at another, each to a carbon atom.

			Symmetry		Bond length / $C–C_p$				
n	Cluster	Spin	Unopt	Opt	C–N	C–B	B–N	N–N	B–B
1	N	$\frac{1}{2}$	T_h	C_{3v}	0.95 (3) 1.32 (1)	—	—	—	—
	B	$\frac{1}{2}$	T_h	C_{3v}	—	1.02 (3) 1.06 (1)	—	—	—
2	N_2	0	D_{3d}	D_{3d}	0.94 (3,3)	—	—	1.43 (1)	—
	B_2	0	D_{3d}	D_{3d}	—	0.99 (3,3)	—	—	1.31 (1)
	BN	0	C_{3v}	C_{3v}	0.99 (3)	1.02 (3)	1.03 (1)	—	—
3	N–B–N	$\frac{1}{2}$	C_{2v}	C_s	0.94 (2) 1.32 (1) 1.00 (2) 0.98 (1)	1.03 (2)	1.03 (1) 0.96 (1)	—	—
	B–N–N	$\frac{1}{2}$	C_s	C_s	0.96 (3) 0.94 (2)	1.02 (3)	0.99 (1)	1.30 (1)	—
	B–N–B	$\frac{1}{2}$	C_{2v}	C_s[a]	0.98 (2)	1.02 (2,2) 1.03 (1,1)	1.02 (2)	—	—
	B–B–N	$\frac{1}{2}$	C_s	C_s	1.00 (3)	1.00 (3,2)	1.01 (1)	—	1.14 (1)
	N_3	$\frac{1}{2}$	C_{2v}	C_s	0.95 (2) 0.96 (1) 0.92 (2) 0.94 (1) 0.89 (2)	—	—	1.40 (1) 1.28 (1)	—
	B_3	$\frac{1}{2}$	C_{2v}	C_{2v}	—	1.00 (2,2) 1.04 (1,1) 0.98 (2)	—	—	—
4	B–BN_2	0	C_s	C_s	1.00 (2,2) 0.98 (1,1)	1.02 (3,1)	1.02 (2)	—	1.04 (1)
	N–NB_2	0	C_s	C_s	1.00 (2) 1.02 (1) 0.98 (1)	1.02 (3,3)	1.02 (2)	1.00 (1)	—
	B–N–B–N	0	C_s	C_s	1.00 (3) 0.98 (2)	1.02 (3,2)	1.03 (2) 1.01 (1)	—	—
	BN_3	1	C_{3v}	C_1	1.02 (3,2,2) 1.06 (1,1)	0.96 (1)	0.99 (2) 1.05 (1)	—	—
	B–NN_2	0	C_s	C_1	0.93 (3,1) 1.03 (1) 1.01 (1) 0.98 (1)	1.02 (3)	0.98 (1)	1.42 (1) 0.93 (1)	—
	NB_3	0	C_{3v}	C_s	0.96 (1)	1.02 (3,2,2) 1.06 (1,1)	0.99 (2) 1.05 (1)	—	—
	N–BB_2	0	C_s	C_s	1.00 (2) 1.01 (1)	1.00 (2,2) 1.07 (1,1) 0.98 (1)	0.97 (1)	—	1.11 (2)
5	BN_4	$\frac{3}{2}$	T_h	C_1	0.94 (2,2,2) 1.33 (1,1,1) 1.00 (3)	—	0.97 (2) 1.06 (1) 0.95 (1)	—	—
	B–NN_3	$\frac{1}{2}$	C_{3v}	C_s	0.94 (3,3) 1.02 (3)	1.02 (2) 1.05 (1)	0.96 (1)	1.33 (2) 0.89 (1)	—
	NB_4	$\frac{3}{2}$	T_h	T_h	—	1.03 (3,3,3,3)	0.99 (4)	—	—
	N–BB_3	$\frac{1}{2}$	C_{3v}	C_s	1.00 (3)	1.00 (2,2) 1.05 (1,1) 1.02 (2) 0.99 (1)	0.94 (1)	—	1.07 (2) 1.19 (1)

[a] C–B bond lengths differ by less than 1%, making the symmetry almost C_{2v}.

The most stable spin state of BN_3 is 1 due to the two extra electrons added by nitrogen atoms not directly bonded to one another. This results in C_s symmetry; one nitrogen has all three of its C–N bonds extended by 2% relative to $C–C_p$ and the other two N atoms have one C–N bond longer still (6%). Unlike BN_3, asymmetric B–NN_2 has a low spin (0) ground state and its symmetry is just C_1. The two distances between the central and outer nitrogen atoms differ hugely: 1.44 and 2.20 Å.

By contrast the boron-rich four atom clusters deviate from high symmetry only slightly. A small shift, mainly in the positions of two B atoms in (spin 0) NB_3, causes a reduction of symmetry from C_{3v} to C_s, retaining one mirror plane. The three boron atoms in N–BB_2 perform a scissor motion during relaxation, maintaining a mirror plane while increasing the interboron distance and reducing the boron–nitrogen bond length.

In its lowest energy state of spin $\frac{3}{2}$, the BN_4 cluster has three nitrogen atoms with one C–N bond far longer than the other two whilst the fourth N remains close to its lattice position. The movement of the three N atoms is accompanied by a shift of the central boron from its three-fold symmetric position. This results in a complete loss of symmetry during relaxation. B–NN_3 is spin $\frac{1}{2}$, also with a symmetry of C_s. Two peripheral nitrogen atoms in B–NN_3 move away from the central N during relaxation, causing mirror symmetric elongations of the two N–N distances and leaving the central nitrogen coordinated to the neighbouring boron and one remaining nitrogen.

Despite sharing the same spin as its nitrogen-rich counterpart, the NB_4 ground-state, unlike BN_4, maintains tetrahedral symmetry with minor strain in all bonds compared to the perfect lattice. The ground state of N–BB_3, on the other hand, is spin $\frac{1}{2}$ and the B–B bond lengths are much the same as in the smaller N–BB_2 cluster, the additional boron atom sitting on the mirror plane in a peripheral position.
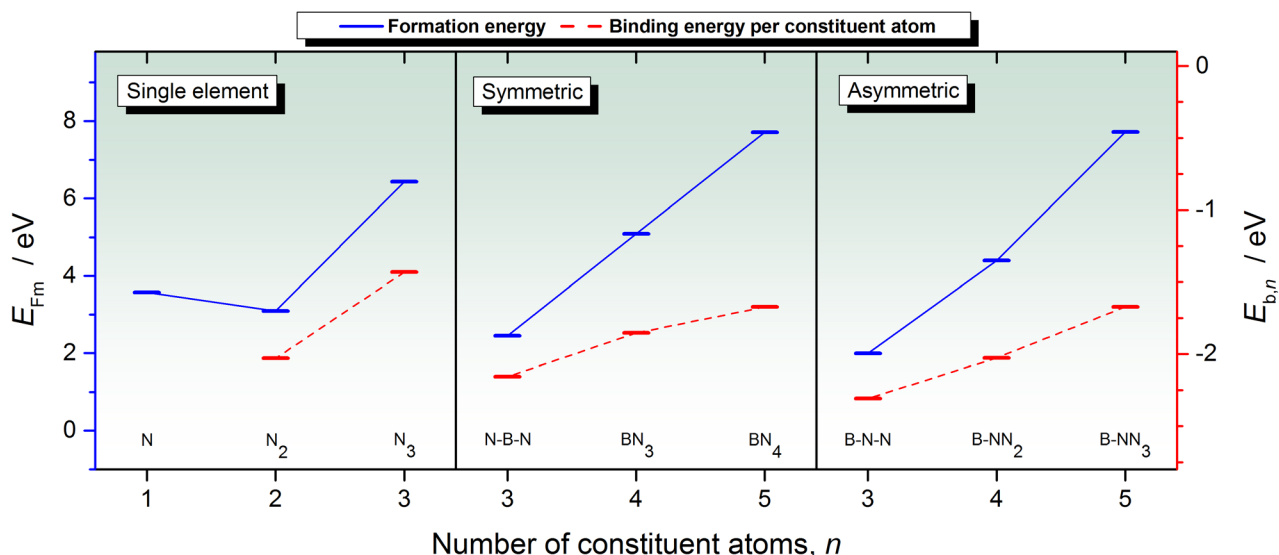
Figure 5. Plots of formation energy E_{Fm} and binding energy per constituent atom $E_{b,n}$ against n for the nitrogen-rich single element, symmetric and asymmetric clusters. Note that the $E_{b,n}$ axis (right) is set to the same range as figure 6, but the E_{Fm} axis (left) is scaled to best represent the E_{Fm} range. Present as guides to the eye, the solid blue and dashed red lines connect E_{Fm} and $E_{b,n}$ values respectively.

3.2. Energetics

In figures 5 and 6 are the HSE-06 structural energetic data for the range of nitrogen-rich and boron-rich defects, respectively, showing both the formation energy (E_{Fm}) and binding energy per constituent atom ($E_{b,n}$). For single N and B dopants only E_{Fm} applies, and the values of 3.58 and 1.77 eV respectively agree well with those published previously [46]. It is important to note that when considering the energetics of N or B atom loss from dopant clusters, we limit our scope to single atom losses since dopants are considered unlikely to migrate in cluster form.

The binding energies of the single-element pairs, N_2 and B_2, are -4.06 and -1.29 eV respectively, also in excellent agreement with the results of previous researchers [41]. The binding energy of N_2 reflects the tendency of type I diamond to accommodate A-centres.

When n increases in single-element clusters from 2 to 3, we find an increase in formation energy and less well-bound clusters. For nitrogen, this is in part due to the formally unsatisfied valencies causing an energetically expensive symmetric distortion of both N–N bonds; in N_2, on the other hand, the valencies are satisfied.

Figure 7 shows the structural energetic data for clusters containing equal numbers of boron and nitrogen atoms. A simple defect with a large binding energy of -5.52 eV and even a negative formation energy of -0.17 eV, the BN defect is a potentially present cluster in multiple types of diamond.

The binding energies of N–B–N and B–N–N differ by 0.46 eV, in agreement with previous work [12]. Addition of further nitrogen atoms to these clusters lowers their binding energy per atom, with the asymmetric case more stable than the symmetric for $n = 4$. By contrast for $n = 5$ the symmetric spin $\frac{3}{2}$ cluster, BN_4, is almost energetically equal to its asymmetric, spin $\frac{1}{2}$, counterpart. Relaxation of three N atoms in BN_4 results in shorter and stronger bonds with both the central boron and two of their three nearest-neighbour carbons.

The asymmetric cluster B–NN_3 does not similarly relax: the central N atom shares no bonds with C atoms so cannot make the single C–N bond elongation made by N atoms in many clusters.

The boron-rich clusters lack the lone pair electron density present in their nitrogen-rich analogues. Positioning a nitrogen atom at the centre of a cluster causes stabilisation with respect to both B_{n-1} plus isolated nitrogen and to clusters with peripheral N atoms for all values of n. Interestingly, the formation energies of the asymmetric clusters for $n = 3$–5 are comparable to those of the $n = 1$–3 single element boron clusters. Once formed however, these clusters are more tightly bound than B_x because of the high energy associated with forming a single N centre. The largest difference in formation energy between two boron-rich clusters that differ in content by one boron atom is 1.82 eV between B_3 and B_2, so that the dissociation of B_3 to form B_2 and B is exothermic by 0.1 eV. All other boron-rich clusters are stable with respect to loss of boron[5].

In general the boron-rich clusters are less distorted than the nitrogen-rich clusters, resulting in lower formation energies, but have similar binding energies due to the accommodation of single nitrogen defects being very endothermic. For both boron- and nitrogen-rich clusters $E_{b,n}$ is largest for $n = 3$, provided they contain an atom of the other element. Comparison of B–BN_2 and N–NB_2 with BN, and N_2 with BN_3 and B–NN_2 shows that the addition of a BN unit usually causes only small changes in $E_{b,n}$ when nitrogen is present in the cluster. B–N–B–N is likely to outnumber its more compact counterparts with the same stoichiometry as its binding energy significantly outweighs theirs; it has the most negative binding energy of any cluster examined here.

The asymmetric N-rich clusters are more stable than the corresponding symmetric clusters for $n = 3$ and 4, and BN_4 and B–NN_3 are almost energetically equal. This may result in

---

[5] Losses of multiple atoms simultaneously are kinetically unlikely so are not considered here.
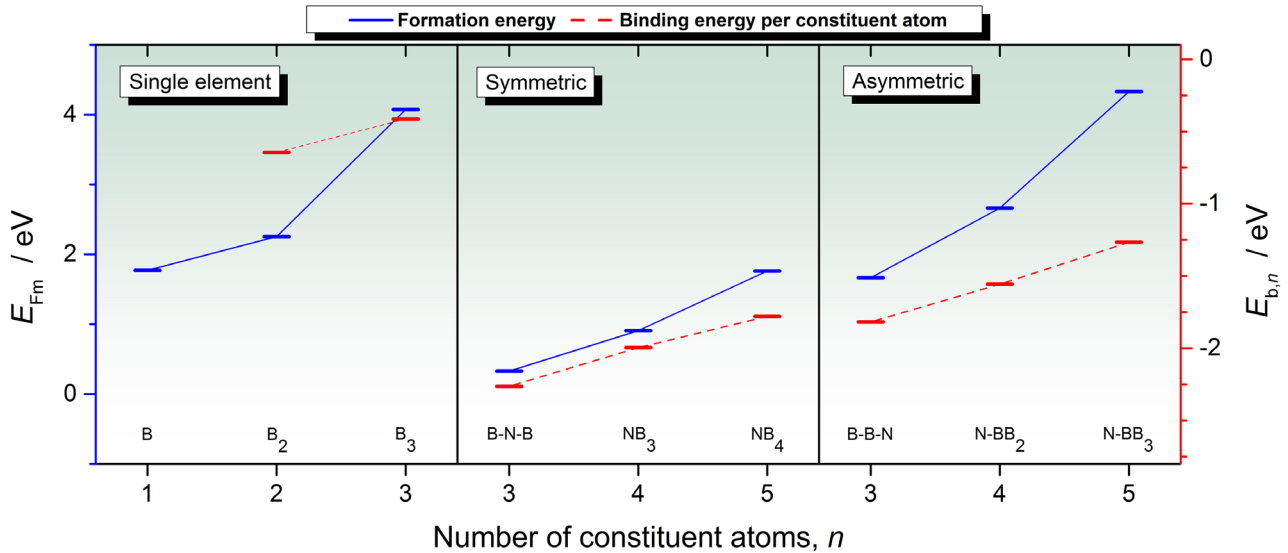
Figure 6. Formation energy E_{Fm} and binding energy per constituent atom $E_{\mathrm{b},n}$ against n for the boron-rich single element, symmetric and asymmetric clusters. Notes on scale and lines are the same as in figure 5.
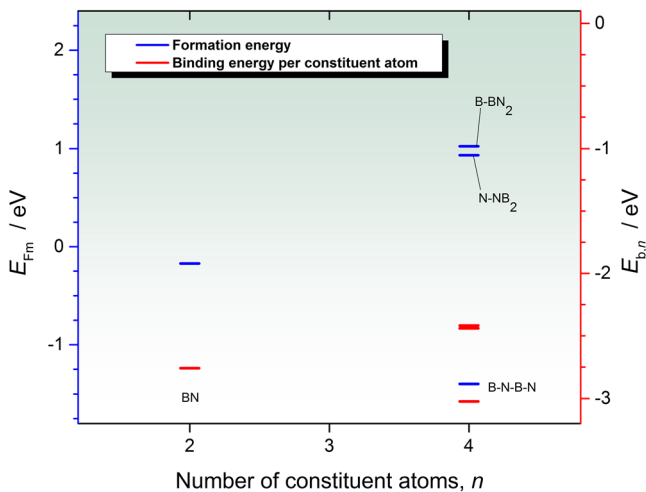
Figure 7. Formation energy E_{Fm} and binding energy per constituent atom $E_{\mathrm{b},n}$ against n for the four equal boron-nitrogen clusters. Notes on colours are the same as in figure 5, but the $E_{\mathrm{b},n}$ scale is different.

Table 2. Excitation energy μ_{e} for various substitutional acceptors (A) and donors (D) in diamond, calculated by both the HSE-06 DOS method and the EMM. 'M' refers to a level producing a metallic DOS from which the value cannot be derived.

Dopant	Type	HSE-06 μ_{e} / eV	EMM μ_{e} / eV	Literature μ_{e} / eV
B	A	M	0.37[a]	0.37, [48]
Al	A	0.94	0.82	1.0, [46]
Li	A	1.48	1.62	1.4, [49]
N	D	1.65	1.70[a]	1.70, [33]
P	D	M	0.74	0.60, [50]
S	D	1.57	1.38	1.2, [51, 52]
O	D	2.18	2.63	2.5–2.7, [52]

[a] Levels used in the EMM as empirical markers.

a greater concentration of BN_4 than its smaller counterparts since, for example, an isomeric rearrangement of BN_3 favourably results in B–NN_2 formation. Given this, there may not be a clear route to BN_4 formation via addition of N atoms to smaller clusters, despite its stability.

Under thermodynamic control and for given appropriate dopant concentrations the clusters with the most negative binding energy will prevail. Considering the tendency of nitrogen to cluster, a co-doped N-rich sample might contain some combination of (for example) N–N–B, B–NN_2, BN_4 and some purely N containing clusters, depending on the ratio of nitrogen to boron.

For boron-rich clusters the structures involve atomic separations and geometries more similar to those in the perfect diamond lattice. This gives both low formation energies and high stabilities of clusters with multiple boron atoms. The low energy required to produce a single boron defect results in the instability of the B_3 complex with respect to loss of B, but all other examined boron-rich clusters lack an exothermic destruction pathway[5]. The symmetric boron-rich clusters are all more stable than the asymmetric clusters. Additionally, unlike their N-rich counterparts the NB_x defects have large E_{b} values relative to the single element defects.

The B_2 cluster may theoretically be bound only up to 750 K [47], but all defects incorporating nitrogen studied here are predicted to have much larger E_{b} values. It is therefore likely that boron-rich co-doped diamond might produce some of the symmetric NB_x clusters with $x = 1$–4 during HPHT preparation, again depending on the boron-nitrogen ratio.

One further consideration for HPHT preparation of these clusters is non-ground-state spin. At the high temperature used, kT will lie in the approximate range 0.15–0.2 eV. NB_3 has spin states (0 and 1) that differ by 0.2 eV, the upper end of this scale. The BN_3 and NB_4 ground-states, spin 1 and $\frac{3}{2}$ respectively, lie below their higher energy spin states by around 2–3 times kT. Each of the other clusters have far larger energy gaps between their spin states, making them unlikely to occupy the higher energy state upon preparation by HPHT.
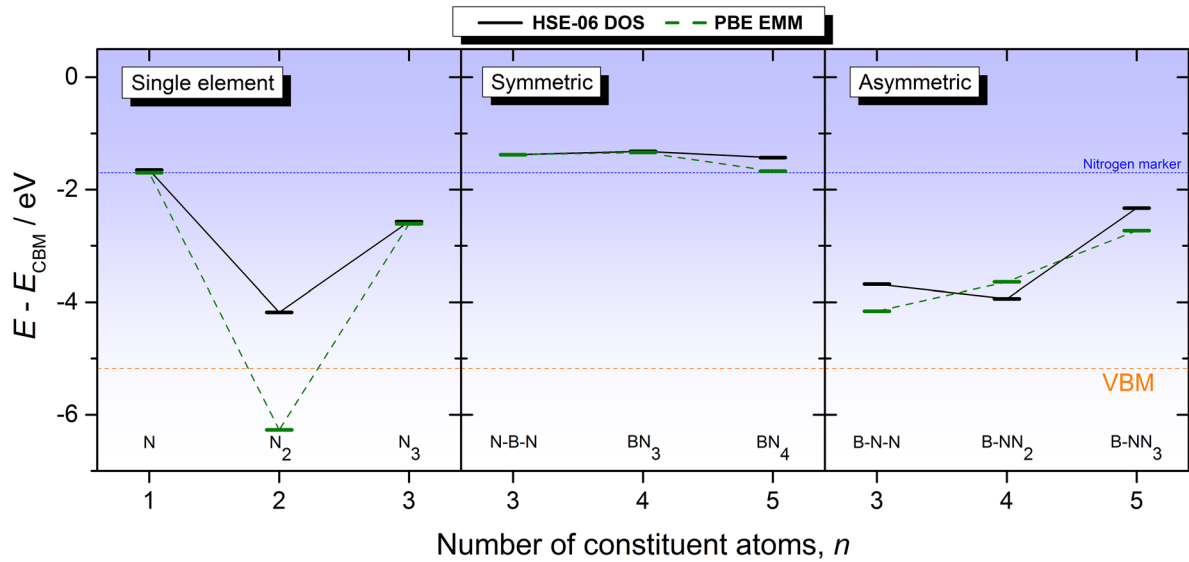
Figure 8. Nitrogen-rich cluster donor levels against *n* for both the HSE-06 density of states method (black solid lines) and the PBE empirical marker method (green dashed lines). The nitrogen EMM marker and the VBM are given for reference.
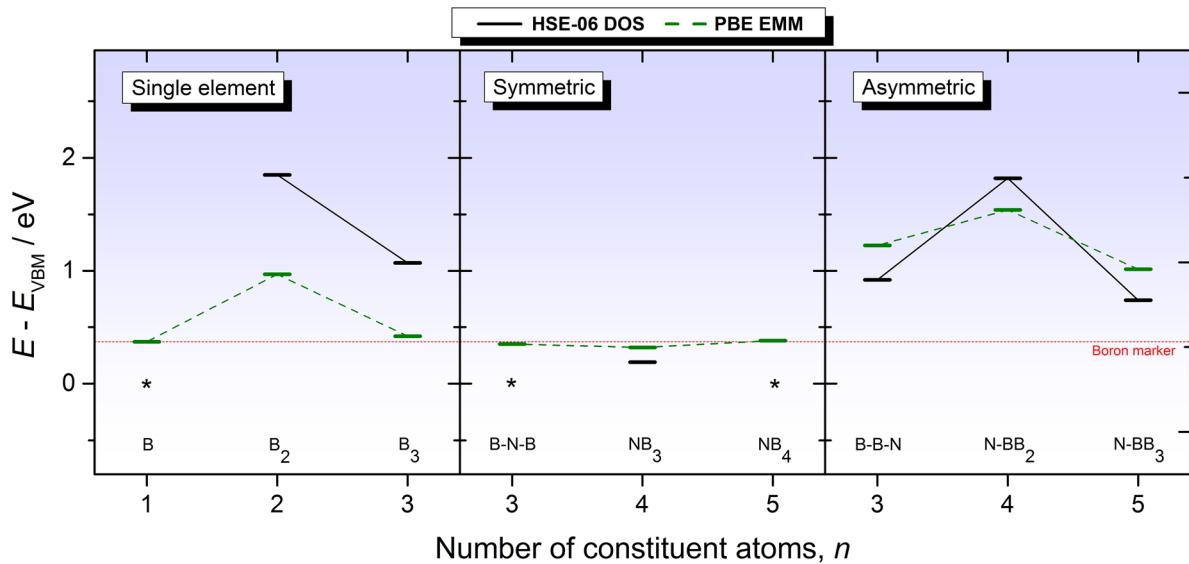
Figure 9. Boron-rich cluster acceptor levels against *n* for both the HSE-06 density of states method (black solid lines) and the PBE empirical marker method (green dashed lines). The boron EMM marker is given for reference. A star denotes a metallic DOS spectrum from which the level cannot be ascertained.

3.3. Excitation energies

CRYSTAL HSE-06 DOS spectra show the difference between the mid-gap levels and the relevant band: the CBM for donors and the valence band maximum (VBM) for acceptors. From these levels the excitation energy of a defect μ_e can be obtained. Advantages of this method include that it relies on no empirical input, so is a truely *ab initio* technique, and that it only provides levels within the band-gap, unequivocally providing results on defects of interest. Disadvantages include the *slightly* narrow diamond band-gap obtained by calculations using HSE-06, here 5.2 eV (compared to 5.5 eV experimentally), increasing the likelihood of metallic DOS spectra. Additionally, unrealistically high impurity concentrations cause degenerate doping; diamond supercells examined

with 1 defect in 512 atoms have concentrations as high as 3.5×10^{20} cm^{-3}.

The EMM results complement the HSE-06 data, and have the advantage that even shallow excitation energies can be obtained. Its comparative nature means calculations on high concentrations can give reasonable results provided the supercell is large enough that charged states do not result in unphysical geometries. Using an experimental marker, it is of course not a truly *ab initio* method.

With their respective advantages and disadvantages, neither of the two methods would be appropriate to consider the large range of defects in this work comprehensively. Whilst the levels obtained from the two methods are rarely identical, they are sufficiently similar that comparison

provides justifiable insight. Table 2 shows the HSE-06 and EMM results for a range of well studied diamond dopants. The combination of both methods is invaluable when considering shallow-level defects, as exemplified by B and P, where the DOS method is unreliable in quantifying the excitation energy.

μ_e of the N-rich donor clusters and B-rich acceptor clusters are shown in figures 8 and 9, where the values are given with respect to the CBM and VBM for donors and acceptors respectively. Excluding those acceptor levels too shallow to determine by the DOS method, the two methods tend to agree well. Values for previously studied examples such as N_2, B_2, N–B–N, and B–N–N are in good agreement with the literature [12, 41].

The trends apparent in the N-rich and B-rich plots somewhat mirror each other. For example, the *pure* elemental defects with $n = 1$–3 show a shallow-deep-medium pattern in both boron and nitrogen. When $n = 2$ two half-spin defects combine to make a zero total spin ground-state, stabilising the associated charge and its band-gap state, thereby requiring more energy to excite an electron either from donor level to conduction band or valence band to acceptor level. The $n = 2$ level is thus deeper than $n = 1$. The $n = 3$ cluster may be considered a 'mixture' of $n = 1$ and 2. This spin dictated progression is also apparent in the boron-rich $n = 3$–5 clusters.

One striking difference between nitrogen-rich and boron-rich clusters is the asymmetric $n = 3$ and 4 clusters. While B–N–N and $B–NN_2$ have similar μ_e, B–B–N has a shallower level than $N–BB_2$. The former is likely to be associated with the smaller structural distortion in B–N–N relative to $B–NN_2$ and its effect on the nitrogen electron density. There is no analogous effect in the boron-rich clusters.

For symmetric nitrogen-rich clusters with $n = 3$–5, addition of N atoms does not significantly reduce μ_e as might be expected. Whereas, in the asymmetric versions each nitrogen addition reduces the donor excitation energy. This difference can be understood by considering N–B–N as $(NB)^0–N^0$ and B–N–N as $B^-–N_2^+$ [12]. Addition of N atoms to the former simply causes further N^0 centres in (very) close proximity to an existing deep donor defect. On the other hand, addition of N atoms to the asymmetric cluster causes further concentration of electron density in the already negative region of the donor cluster. This stacking of negative charge pushes the associated level to higher energies and makes donation of an electron more favourable.

As donors, the symmetric N-rich clusters have similar μ_e values to the single nitrogen centre and the asymmetric N-rich clusters have deep levels. With the range of defects that could be present, a HPHT prepared material would maintain a range of levels within the band-gap, which if detectable may be difficult to interpret.

μ_e for the boron-rich clusters are all lower than the equivalent nitrogen-rich defects. The band-gap levels of the stable symmetric clusters would even be similar to that of the single boron impurity, so might be indistinguishable by some experimental techniques. These defects could already exist in some natural or HPHT type II-b diamond.

4. Conclusions

In this paper, we have analysed a broad range of substitutional boron-nitrogen co-dopant clusters by means of hybrid DFT calculations. We have examined ground-state geometries and both structural and electronic energies in detail. HSE-06 electronic energy levels are in good agreement with those determined by the EMM using the GGA. Trends in the energies are discussed in terms of charge and structure.

The electron density in the nitrogen-rich clusters leads to large local geometric distortions, low symmetries, high formation energies and deep band-gap states. Nevertheless, nitrogen-rich clusters are strongly bound and, apart from the $B–NN_3$ cluster, are stable with respect to loss of nitrogen. Depending on preparation conditions, the asymmetric N-rich clusters will play a part in nitrogen-rich co-doped material. In contrast, the boron-rich clusters lead to smaller bond length changes compared to pure diamond, are all (apart from B_3) stable with respect to loss of boron atoms[5] and to formation of pure boron clusters. Those of highest stability, NB_x, have electronic energy levels comparable to that of B.

With respect to n-type diamond, it is clear that B-rich co-doping would be detrimental. Whilst BN_2 and BN_3 appear to be the strongest candidates examined here, there is no clear advantage over other well-known donor dopants such as phosphorus. Moreover, their asymmetric counterparts are both more stable and produce deeper lying energy levels.

We hope this work will stimulate further studies of co-dopants, both experimentally in realisation of clusters by HPHT treatment and detection by (e.g.) solid-state magnetic resonance or core-level spectroscopy, and theoretically in the increasingly comprehensive understanding of further combinations of elements in diamond.

Acknowledgments

ORCID iDs

Alex Croot ● https://orcid.org/0000-0001-5469-6427
Sergio Conejeros ● https://orcid.org/0000-0002-2490-1677
Neil A Fox ● https://orcid.org/0000-0003-1608-1485
Neil L Allan ● https://orcid.org/0000-0001-9342-6198

References

[1] Thonke K 2003 *Semicond. Sci. Technol.* **18** S20
[2] Kalish R 2001 *Diam. Relat. Mater.* **10** 1749–55
[3] Katagiri M, Isoya J, Koizumi S and Kanda H 2004 *Appl. Phys. Lett.* **85** 6365
[4] Yu B D, Miyamoto Y and Sugino O 2000 *Appl. Phys. Lett.* **76** 976
[5] Barnard A S, Russo S P and Snook I K 2003 *Phil. Mag.* **83** 1163–74
[6] Katayama-Yoshida H, Nishimatsu T, Yamamoto T and Orita N 2001 *J. Phys.: Condens. Matter* **13** 8901
[7] Katayama-Yoshida H, Nishimatsu T, Yamamoto T and Orita N 1998 *Phys. Status Solidi* B **210** 429–36
[8] Segev D and Wei S H 2003 *Phys. Rev. Lett.* **91** 126406
[9] Moussa J E, Marom N, Sai N and Chelikowsky J R 2012 *Phys. Rev. Lett.* **108** 226404
[10] Goss J P, Briddon P R and Eyre R J 2006 *Phys. Rev.* B **74** 245217
[11] Othman M Z, Conejeros S J, Croot A, O'Donnell K M, Hart J N, May P W and Allan N L in preparation
[12] Eyre R J, Goss J P, Briddon P R and Wardle M G 2007 *Phys. Status Solidi* A **204** 2971–7
[13] Butler J E, Mankelevich Y A, Cheesman A, Ma J and Ashfold M N R 2009 *J. Phys.: Condens. Matter* **21** 364201
[14] Teraji T, Wada H, Yamamoto M, Arima K and Ito T 2006 *Diam. Relat. Mater.* **15** 602–6
[15] Saguy C 2004 *Defect Diffus. Forum* **226** 31–48
[16] Yagi I, Tsunozaki K, Fujishima A, Ohtani B and Uosaki K 2002 *J. Electrochem. Soc.* **149** E1
[17] Silva L L G, Trava-Airoldi V J, Corat E J, Added N and Sumodjo P T A 2007 *Diam. Relat. Mater.* **16** 174–80
[18] Sonoda S, Won J H, Yagi H, Hatta A, Ito T and Hiraki A 1997 *Appl. Phys. Lett.* **70** 2574–6
[19] Locher R, Wagner J, Fuchs F, Wild C, Hiesinger P, Gonon P and Koidl P 1995 *Mater. Sci. Eng.* B **29** 211–5
[20] Freitas J A, Doverspike K, Klein P, Khong Y and Collins A 1994 *Diam. Relat. Mater.* **3** 821–4
[21] Othman M Z, May P W and Fox N A 2012 *MRS Proc.* **1511** Mrsf12-1511-ee05-05
[22] Halliwell S C, May P W, Fox N A and Othman M Z 2017 *Diam. Relat. Mater.* **76** 115–22
[23] Hu X J, Li R B, Shen H S, Dai Y and He X 2004 *Carbon* **42** 1501
[24] Evans T, Qi Z and Maguire J 1981 *J. Phys. C: Solid State Phys.* **14** L379
[25] Isoya J, Kanda H and Morita Y 1997 *Phys. Rev.* B **56** 6392
[26] Ishii N and Shimizu T 1998 *Phys. Rev.* B **58** 12533
[27] Li Y, Jia X, Shi W, Leng S, Ma H A, Sun S, Wang F, Chen N and Long Y 2014 *Int. J. Refract. Met. Hard Mater.* **43** 147–9
[28] Yan B, Jia X, Sun S, Zhou Z, Fang C, Chen N, Li Y, Li Y and Ma H A 2015 *Int. J. Refract. Met. Hard Mater.* **48** 56–60
[29] Mao W, Liu Y H, Wen-feng G, Ling-sheng W, Zhi L, Yamei W and Ruixia Y 2016 *Chin. Phys. Lett.* **33** 028101
[30] Goss J P, Eyre R J and Briddon P R 2008 *Phys. Status Solidi* B **245** 1679–700
[31] Hu X J, Dai Y B, Shen H S and He X C 2005 *Physica* B **367** 86–91
[32] Kaiser W and Bond W L 1959 *Phys. Rev.* **115** 857–63
[33] Lombardi E B, Mainwood A, Osuch K and Reynhardt E C 2003 *J. Phys.: Condens. Matter* **15** 3135–49
[34] Dovesi R *et al* 2014 *Int. J. Quantum Chem.* **114** 1287–317
[35] Heyd J, Scuseria G E and Ernzerhof M 2003 *J. Chem. Phys.* **118** 8207–15
[36] Catti M, Pavese A, Dovesi R and Saunders V R 1993 *Phys. Rev.* B **47** 9189–98
[37] Peintinger M F, Oliveira D V and Bredow T 2013 *J. Comput. Chem.* **34** 451–9
[38] Monkhorst H J and Pack J D 1976 *Phys. Rev.* B **13** 5188
[39] Pfrommer B G, Cote M, Louie S G and Cohen M L 1997 *J. Comput. Phys.* **131** 233–40
[40] Liberman D A 2000 *Phys. Rev.* B **62** 6851–3
[41] Goss J P, Eyre R J and Briddon P R 2008 *J. Phys.: Condens. Matter* **20**
[42] Perdew J P, Burke K and Ernzerhof M 1996 *Phys. Rev. Lett.* **77** 3865
[43] Clark S, Segall M, Pickard C, Hasnip P, Probert M, Refson K and Payne M 2005 *Z. Kristallogr. Cryst. Mater.* **220** 567–70
[44] Vanderbilt D 1990 *Phys. Rev.* B **41** 7892
[45] Miyazaki T, Okushi H and Uda T 2002 *Phys. Rev. Lett.* **88** 66402
[46] Czelej K, Śpiewak P and Kurzydowski K J 2017 *Diam. Relat. Mater.* **75** 146–51
[47] MacLeod R, Murray S, Goss J, Briddon P and Eyre R 2009 *Phys. Rev.* B **80** 054106
[48] Crowther P A, Dean P J and Sherman W F 1967 *Phys. Rev.* **154** 772–85
[49] Goss J P and Briddon P R 2007 *Phys. Rev.* B **75** 075202
[50] Gheeraert E, Koizumi S, Teraji T and Kanda H 2000 *Solid State Commun.* **113** 577–80
[51] Miyazaki T and Okushi H 2001 *Diam. Relat. Mater.* **10** 449–52
[52] Goss J P, Briddon P R, Jones R and Sque S 2004 *Diam. Relat. Mater.* **13** 684–90
[53] Momma K and Izumi F 2011 *J. Appl. Crystallogr.* **44** 1272–6